Critical Exponents for Line Tension and Dipole Density Difference from Lipid Monolayer Domain Boundary Fluctuations

5 AUTHORS, INCLUDING:

Ilya Levental
University of Texas Health Science Center …
49 PUBLICATIONS   2,235 CITATIONS

SEE PROFILE

Hannah Gelman
University of Illinois, Urbana-Champaign
8 PUBLICATIONS   104 CITATIONS

SEE PROFILE

Paul Janmey
University of Pennsylvania
349 PUBLICATIONS   25,174 CITATIONS

SEE PROFILE

Tobias Baumgart
University of Pennsylvania
95 PUBLICATIONS   3,597 CITATIONS

SEE PROFILE

Article

Critical Exponents for Line Tension and Dipole Density Difference from Lipid Monolayer Domain Boundary Fluctuations

Michael C. Heinrich, Ilya Levental, Hannah Gelman, Paul A. Janmey, and Tobias Baumgart

More About This Article

Additional resources and features associated with this article are available within the HTML version:

- Supporting Information
- Access to high resolution figures
- Links to articles and content related to this article
- Copyright permission to reproduce figures and/or text from this article

View the Full Text HTML

Critical Exponents for Line Tension and Dipole Density Difference from Lipid Monolayer Domain Boundary Fluctuations

Michael C. Heinrich,[†,‡] Ilya Levental,[§,‡] Hannah Gelman,[∥] Paul A. Janmey,[§] and Tobias Baumgart*,[†]

Department of Chemistry, Institute for Medicine and Engineering, and Laboratory for Research on the Structure of Matter, University of Pennsylvania, 231 South 34th Street, Philadelphia, Pennsylvania 19104

The potential physiological relevance of liquid−liquid phase separation in lipid membranes to the formation and stability of "lipid rafts" in cellular plasma membranes has prompted extensive investigation of the physical chemistry underlying these phenomena. In this contribution, the line tension (γ) and dipole density differences (μ) between demixed fluid phases of monolayers comprised of dimyristoylphosphatidylcholine (DMPC) and dihydrocholesterol (DChol) were investigated by measuring the two-dimensional thermal fluctuations of domain boundaries visualized by the inclusion of a fluorescent tracer lipid. These parameters are essential determinants of domain stability, and their quantification will yield an increased understanding of the physical processes responsible for aspects of lateral phase separation. Employing an extensive data set, the surface pressure dependence of γ and μ was determined at three different monolayer compositions (30%, 35%, and 40% DChol). Both parameters were found to decrease with a power law dependence as the surface pressure approached the phase transition pressure (π_t), in agreement with previous measurements. Additionally, photobleaching effects and domain size influence were quantified and found to be small in our system. We suggest that the method of flicker spectroscopy can be helpful in identifying line-active compounds.

Introduction

In recent years, lateral compositional heterogeneities in lipid membranes have received significant interest because of speculation about their involvement in signaling and trafficking complexes in cellular membranes. In particular, the "membrane raft" hypothesis[1] has stimulated in-depth studies of liquid−liquid phase separation in multicomponent lipid membranes. Microscopically visible phase separation has been demonstrated in both mixed bilayer[2–5] and monolayer systems,[6,7] and the physical chemistry of phase separation in both bilayers[8] and monolayers[9,10] has been investigated extensively. Fluid phase coexistence in lipid bilayer membranes is characterized by the formation of a liquid ordered (L_o) phase, associated with a higher degree of lateral ordering/packing than the liquid disordered (L_α or L_d) phase observed in pure phospholipid membranes and was first demonstrated by Dietrich et al.[2] and Samsonov et al.[3] Fluid phase coexistence in lipid monolayers was first observed by Subramaniam et al.[11] Of particular interest is the characterization of transitions from two observable immiscible phases to a single homogeneous phase. These mixing/demixing transitions have been shown to be functions of lipid composition,[12] temperature,[13–15] surface pressure,[16,17] and degree of cross-linking,[18] while compositional fluctuations on length scales below optical resolution are also beginning to be addressed.[19–23] Recent observation of qualitatively similar liquid−liquid phase separation in plasma membrane-derived giant vesicles (GPMVs) has further underlined the potential biological relevance of these model membrane findings.[24]

Of particular interest is the question of how domain size is regulated.[25] In lipid bilayer membranes, the only known driving force for domain coarsening is line tension at the phase boundary. Quantification of this parameter is helpful not only for understanding domain coarsening kinetics and thermodynamics, but also to elucidate three-dimensional modulation of membrane shape, both in model membranes[13,26,27] and possibly extended to biologically relevant membrane shape transitions related to membrane trafficking.[28] Additionally, variation of the interfacial line tension by membrane minority components would suggest line active species that function as domain stabilizers or disruptors in model systems, and possibly as "lipid raft" regulators in plasma membranes of living cells.

Line tension at liquid domain boundaries has previously been examined both theoretically and experimentally in monolayers[29–32] and in bilayers.[13,27,33,34] We have recently obtained extremely small line tensions in fluctuating lipid bilayer domains of giant unilamellar vesicles.[33] Giant vesicles, typically in the size range of a few dozen micrometers in diameter, pose significant challenges to the accurate analysis of experimental domain undulations due to the spherical geometry that is imaged in the planar focal plane.[33] Lipid monolayers, however, are not limited in lateral dimensions, and their optically flat surface is advantageous for extended flicker spectroscopy studies. In monolayers of 30% cholesterol and 70% dimyristoylphosphatidylcholine (DMPC), line tension was estimated by Benvegnu and McConnell through the relaxation rate following mechanical deformation of bola-shaped domains to the energy minimizing circular domain shape[29] (also see refs 35–37). This study demonstrated monolayer domain line tension to vary by 2 orders of magnitude (from ∼0.1 pN to more than 10 pN) depending on the monolayer surface pressure. A potential limitation of this early work was the need for several secondary parameters and simplifying assumptions in order to analyze the experimental data to yield

* Corrsponding author. E-mail: baumgart@sas.upenn.edu.
† Department of Chemistry.
‡ Authors contributed equally.
§ Institute for Medicine and Engineering.
∥ Laboratory for Research on the Structure of Matter.

line tensions.[29] The dipole density difference between coexisting phases was previously determined in experiments separate from line tension studies via measurements of the diffusional mobility of electrostatically trapped domains,[38] as well as through field-gradient electrophoresis.[39]

Fourier power spectra of thermal domain boundary fluctuations, observable at relatively small line tension, had first been published by Seul and Sammon.[40] Goldstein and Jackson (GJ) then adapted a theory previously developed for magnetic films with phase coexistence[41] to the ultrathin film limit of lipid monolayers with dipolar interactions.[30] The GJ theory relates the competing effects of interfacial line tension and dipolar repulsion to thermal domain boundary in-plane undulations and allowed analysis of the data of ref 40 to yield line tension γ and dipolar density difference μ close to the critical pressure, for a single pressure and composition.[30] Stottrup et al. recently extended these early measurements;[32] their analysis, however, neglected the potentially important dipolar interaction which can modulate the power spectra of domain edge fluctuations. We recently experimentally demonstrated that, in fluctuating lipid bilayer domains, dipolar contributions to the fluctuation spectra are not discernible, as expected from the screening effect due to the existence of an additional aqueous half-space.[33] However, the data presented here, in combination with the GJ analysis, not only show that, in monolayers, dipolar interactions significantly modify fluctuation spectra, but also demonstrate that dipolar interactions can be accurately quantified by flicker spectroscopy.

In this contribution, we extend these findings by applying the GJ theory to the analysis of a large data set of time-lapse images of demixed monolayers to accurately quantify both the line tension and the dipole density difference between the two coexisting liquid phases as a function of surface pressure without external perturbation. Using this approach, we find excellent agreement with published values for γ and μ at 30% DChol; we also determine these parameters in mixtures with 35% and 40% DChol. We furthermore obtain critical exponents for γ and μ as the surface pressure approaches the critical pressure where phase coexistence disappears and again find good agreement with predicted values. To our knowledge, this is the first concurrent quantification of both the line tension and dipole density differences in coexisting fluid phases in lipid monolayers as a function of surface pressure.

Capillary Wave Theory

It has been shown by several authors[30,42,43] that a Fourier ansatz for the shape of a fluctuating domain parametrized in terms of radius R and polar angle θ:

$$R(\theta) = R_0 + \zeta_n \sum_n \cos n\theta \tag{1}$$

yields the excess energy (relative to a nonfluctuating domain) of a fluctuation mode with number n. This excess energy is obtained to second order in mode amplitudes ζ_n as

$$E_n = \frac{1}{2}\Omega_n \zeta_n^2 \tag{2}$$

Here, Ω_n is a restoring force constant for the mode n. In the case of lipid monolayers, it includes contributions from line tension γ at the phase boundary, and the dipole density difference between coexisting phases, μ. Stone and McConnell[44] express the force constant as

$$\Omega_n = \frac{\pi\mu^2(n^2-1)}{R_0}\ln\frac{R_n}{R_0} \tag{3}$$

Here, the equivalent radius R_0 is related to the domain area A by $R_0 = (A/\pi)^{1/2}$. The radius R_n is a value above which a domain with circular ground state will become unstable toward a distortion to a ground state with n-fold symmetry.[42,43,45] R_n is a function of γ, as well as a (generally unknown) microscopic cutoff in terms of the separation distance of adjacent lipid molecules.[42,43,45] An alternative expression for the force constant results from the thin film limit of a theory developed for magnetic layers with phase coexistence:[30,41]

$$\Omega_n = \frac{\pi\gamma}{R_0}\beta_n \tag{4}$$

where β_n is a function of γ and μ and also depends on a "smooth cutoff" in terms of the film thickness h:[30,46]

$$\beta_n = \left[1 - \frac{1}{2}N_B \ln\left(\frac{8R_0}{eh}\right)\right](n^2-1) - \frac{1}{4}N_B(1-4n^2)\sum_{j=2}^n \frac{1}{2j-1} \tag{5}$$

In eq 5, the so-called Bond number N_B is defined as $N_B = 2\mu^2/\gamma$. More generally, the Bond number is a dimensionless number in the theory of fluid mechanics expressed as the ratio between a quantity proportional to fluid density difference (here dipole density difference) and interfacial tension (here line tension). Many properties, including domain shape stability, depend sensitively on the value of N_B.[45]

Both eq 3 and eq 4 yield for the limit of $\mu = 0$ the relation $\Omega_n = \pi\gamma(n^2 - 1)/R_0$, which is found for fluctuations of lipid bilayer domains where measurable dipolar interactions are absent.[33] Both eq 3 and eq 4 account for the conserved area of the fluctuating domain. Note that the form of β_n in refs 30 and 47 contains a sign error (R. Goldstein, personal communication).

Both eq 3 and eq 4 can be used to determine line tension γ and dipole density difference, μ. Hence, values of these parameters from Fourier analysis of fluctuating domains are model dependent. Below, we will focus on using the second approach (eq 4). This allows comparison with the results in ref 30 and enables us to benefit from the fact that the dependence of fit results on the "smooth cutoff"; that is, the film thickness h has been discussed and found to be small.[30] In all subsequent analysis below, we assume $h = 1$ nm.[30]

For the case of $N_B = 0$, that is, zero dipole density difference, the ratios of averaged mode powers given by the second mode $\langle\zeta_2^2\rangle$ divided by higher modes $\langle\zeta_n^2\rangle$, will yield a straight line with slope 1/3 when plotted against $n^2 - 1$.[30,33] If $N_B > 0$, however, the same plot will show deviations from the 1/3 slope which increase with N_B, as we experimentally demonstrate in Figure 1A,D,E. The dependence of N_B values on film pressure for the composition of 30% DChol is shown in Figure 1E. As expected,[29,30] N_B increases as the film pressure approaches the critical pressure (of 10.1 mN/m for our system).

Equation 5 defines conditions for the stability of the circular ground-state shape toward transitions to ground states of different symmetry.[30,42,43,45] With increasing Bond number, the first instable mode is found for $n = 2$, and from eq 5, the critical Bond number below which the circular shape is stable is obtained[30]

$$N_B^*(2) = \frac{2}{\ln(8R_0/h) - 11/6} \tag{6}$$

Note that this critical Bond number is dependent on domain radius, whereas N_B is not. Alternatively, for fixed Bond number,

Lipid Monolayer Domain Boundary Fluctuations

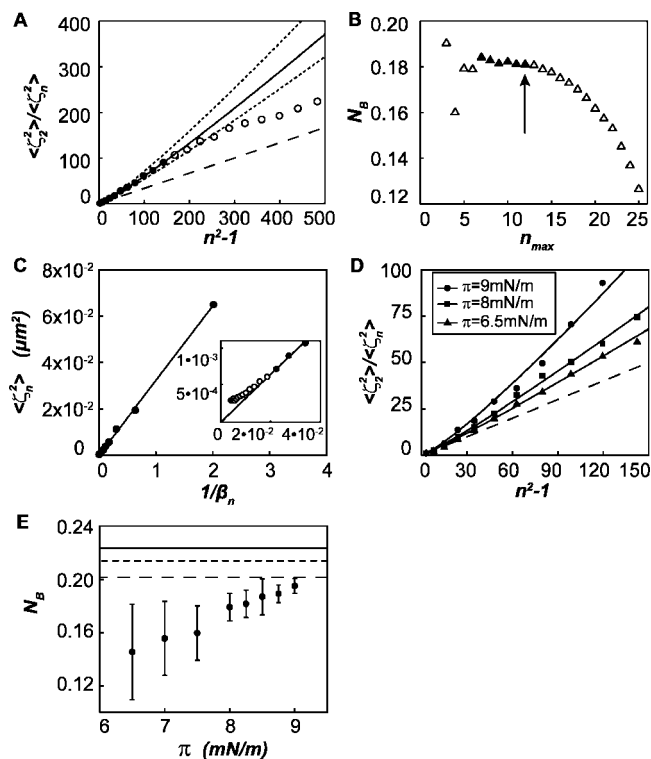*J. Phys. Chem. B, Vol. 112, No. 27, 2008* **8065**

Figure 1. Analysis of mode power fluctuation spectra exemplified for the composition of 30 mol % DChol. (A) FFT-determined mode power ratios $\langle \zeta_2^2 \rangle / \langle \zeta_n^2 \rangle$ for a single domain of radius 7.8 μm at a pressure of 8.25 mN/m at the critical composition. Closed circles are values of $\langle \zeta_2^2 \rangle / \langle \zeta_n^2 \rangle$ where n is an element in the mode set $[n]^*$ included in analysis (see text for details), while open circles have n values larger than n_{max}^*. The dashed line indicates a slope of 1/3. The solid line represents the β_n / β_2 fit to the optimal mode set $[n]^*$, while the dotted lines represent changes in the fit parameter N_B by $\pm 5\%$ to indicate fit quality. (B) Fit parameter N_B of the same domain as in A as a function of mode set considered, as defined by $[n] = [2,..., n_{max}]$. The largest mode set referring to n_{max}^* is indicated by an arrow. Closed triangles represent mode sets large enough to minimize noise, but that also excludes higher modes distorted by aliasing and other distorting effects. (C) Mode powers, $\langle \zeta_n^2 \rangle$, of the same domain as in A are plotted against $1/\beta_n$ using the N_B value from the fit shown in A. Excellent agreement to a linear fit is seen for the modes included in the set $[n]^*$ (closed circles directly related to those in A), but deviation from linearity is found at higher modes (open circles), which are excluded from analysis. The slope of the linear plot is proportional to line tension (see text). (D) FFT-determined mode power ratios $\langle \zeta_2^2 \rangle / \langle \zeta_n^2 \rangle$ for three individual domains at pressures of 6.5, 8, and 9 mN/m at the critical composition. Deviation from the 1/3 slope line (dashed) is seen to increase as the pressure approaches the critical pressure. (E) Average values of N_B as a function of surface pressure for the critical composition. Also plotted are the 2nd mode critical Bond numbers, $N_B^*(2)$ (see eq 3), for domains of radii equal to 16 (dashed line), 9 (dotted line), and 6 μm (solid line), referring to the largest, the average, and smallest domain size in analysis, respectively. N_B is seen to increase with pressure but remains below $N_B^*(2)$ for all domains considered in this contribution.

eq 6 can be used to define a critical radius above which circular domains are instable.[30,42,43,45] All fluctuation spectra examined in the present contribution were obtained from domains with N_B values below the critical Bond number defined by eq 6. Figure 1E shows for the example of 30 mol% DChol that all N_B values remained below the range of critical Bond numbers for the experimental domains considered for this composition. For the condition $N_B < N_B^*(2)$, the assumption of thermal equipartitioning, that is, an energy of 1/2 $k_B T$ per fluctuation mode yields the following expression for the mode amplitudes:[30]

$$\langle \zeta_n^2 \rangle = \frac{k_B T R_0}{\pi \gamma \beta_n} \qquad (7)$$

where k_B is Boltzmann's constant. Note that thermal energy equipartitioning requires the experimental realization of quadratic degrees of freedom (eq 2), which will lead to a Gaussian probability distribution of mode amplitudes. We recently confirmed this condition in fluctuating bilayer domains.[33]

Materials and Methods

Monolayer Manipulation and Visualization. Dimyristoylphosphatidylcholine (DMPC), dihydrocholesterol (DChol), and rhodamine-labeled dioleoylphosphatidylethanolamine (rhoPE) were obtained as chloroform solutions (10 mg/mL) from Avanti (Alabaster, AL). Lipid concentrations were verified by phosphate analysis following acid digestion of organic components[48] and subsequently confirmed by comparison of pure component monolayer isotherms with published data.[49,50] Lipid solutions were prepared immediately prior to the experiment and doped with a trace amount of fluorescent lipid analog (0.5% rhoPE) for visualization. Experiments were conducted at room temperature (~20 °C) with a subphase composed of phosphate buffered saline (PBS: 7.5 mM phosphate, 140 mM NaCl) at pH 7.4 with 5 mM dithiothreitol (Sigma, St. Louis, MO) to prevent oxidation of lipids.

For monolayer experiments, a Langmuir trough (MicroTroughX, Kibron Inc., Helsinki, Finland) was filled with ~25 mL of PBS. Approximately 10 nmol of lipid solution was applied to the subphase−air interface with a glass syringe. The height of the surface was then adjusted by withdrawing subphase from beyond the monolayer barriers until the monolayer could be visualized with an inverted microscope (IX81; Olympus, Center Valley, PA) with a 60× 1.1 numerical aperture long-working distance water immersion objective with coverslip correction (Olympus), a Texas Red filter cube (Chroma, Rockingham, VT), and a back-illuminated electron multiplying charge-coupled device (EM-CCD) camera (ImageEM; Hamamatsu, Bridgewater, NJ). Images were taken at a pixel resolution of 256 × 256 and an exposure time of 0.016 s/frame, yielding an average frame rate of 60 fps, accounting for the finite readout time. The pixel edge size was set at 0.264 μm, close to the optical point spread function width of the microscope.

The monolayer was first compressed quickly (25 Å²/molecule/minute) through the transition pressure while the surface pressure was monitored using the Wilhelmy method[48] and the FilmWare software package (Kibron). The transition pressure was recorded as the last pressure at which inhomogeneity could still be observed under our experimental conditions. After allowing for 5 min of stabilization, the surface pressure was reduced at 5 Å²/molecule/minute to the highest pressure where stable domains could be observed. As Figure 1E exemplarily indicates, our highest pressures were always below the pressures at which domain shape instabilities are expected.[30,42,43,45] For each film pressure, several >2000-frame movies were obtained while slow monolayer flow during the imaging process was compensated for by manual translation of the microscope stage supporting the monolayer trough.

Data Analysis. All image processing was performed using MATLAB (The Mathworks, Natick, MA). Our code allowed selection of individual domains in multidomain frames with a click of a mouse; the tracing routine automatically centered and cropped to the neighborhood around the same identified domain in all subsequent frames, thus allowing tracking and localization frame by frame. The original gray scale images were converted

to binary via thresholding, and the domain boundary for each image was determined from the binary frames and parametrized as the radius function $r(\theta)$, where θ is the polar angle. Image frames where the area of the domain changed by more than 3% were discarded. Area changes of those magnitudes were attributed to motion blur, departure of the domain from the field-of-view due to flow or diffusion, or other imaging artifacts. From the domain area, A, the equivalent radius $R_0 = (A/\pi)^{1/2}$ was obtained. R_0 therefore refers to the radius of a nonfluctuating domain with equal area.

Trace analysis was performed as previously described.[30,33,40,51] The mode powers ζ_n^2 (in units of square micrometers) were determined through fast Fourier transform (FFT) of the individual traces on a frame-by-frame basis and then frame averaged for each domain. Specifically, the radial deviation $\Delta r(\theta) = r(\theta) - \langle r(\theta) \rangle$, where $\langle r(\theta) \rangle$ is the average radius, was Fourier transformed. Note that this average radius is not the same as the equivalent radius R_0 if the domain is fluctuating.[33] We have previously discussed the influence of total frame number included in subsequent analysis.[33] The determination of dipolar effects requires us to obtain average mode powers with high statistical significance. We therefore determined mode powers from averaging FFT data for 1000 frames per domain. An example of averaged mode powers as a function of mode number is given in Figure 1A. Note that, contrary to bilayer spectra, a significant upward deviation from the 1/3 slope discussed above is observed, confirming the findings of Goldstein and Jackson.[30] The set of unitless ratios β_n/β_2 was then fit to the experimentally determined mode power ratios $\langle \zeta_2^2 \rangle / \langle \zeta_n^2 \rangle$ by varying the single fit parameter N_B (Figure 1A). This procedure was repeated for all mode sets $[n] = [2,..., n_{max}]$, where n_{max} ranged from 3 to 25, resulting in 23 potentially different values of N_B. These N_B values were plotted as a function of n_{max}, (see Figure 1B), and the largest mode set prior to a drop-off in the magnitude of N_B was taken to include all resolvable modes for that domain (Figure 1B). This mode set $[n]^* = [2,..., n_{max}^*]$ and its corresponding N_B value were used in all subsequent analyses. The range of modes included for analysis in the example of Figure 1 is indicated by filled symbols in Figure 1A,C, as opposed to open ones that indicate excluded data points, and is further indicated by an arrow in Figure 1B. The rationale for this analysis procedure is the fact that mode powers associated with higher mode numbers $n > n_{max}^*$ will be increasingly distorted through the effects of image pixelization, optical resolution limit, and averaging of domain motion due to finite frame acquisition times.[33] Additionally, mode sets that are too small do not contain enough data points to yield sufficiently accurate N_B values (Figure 1B, open symbols on the lefthand side). The maximum number of resolvable modes depends on the size of fluctuation amplitudes.

With both $[n]^*$ and N_B determined for each individual domain, the mode powers $\langle \zeta_n^2 \rangle$ were plotted against $1/\beta_n$ (see Figure 1C) and a least-squares linear fit to the form $y = mx$, with a slope, m, equal to $kTR_0/\pi\gamma$ (eq 7), yielded the line tension. Small values of $1/\beta_n$, referring to large mode numbers ($n > n_{max}^*$) showed a progressive upward deviation from the expected linear relation (see open symbols in the inset of Figure 1C) and were not included in the analysis. Finally, the dipole density difference μ was obtained from the Bond number N_B via $N_B = 2\mu^2/\gamma$. Approximately 10 domains at each pressure and composition were analyzed to obtain average values of γ and μ^2 (typically for mode power analysis of the first 1000 frames in an image sequence only, except where mentioned below).
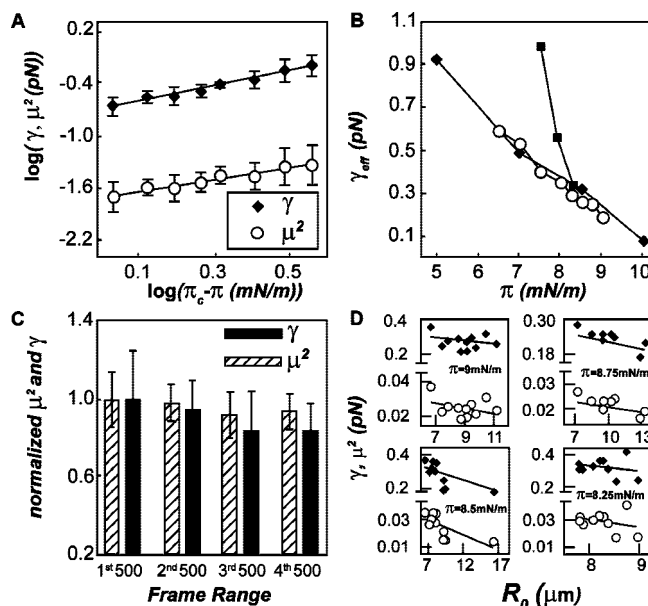

Figure 2. Line tension and dipole density differences at critical composition. (A) Log of γ (filled diamonds) and μ^2 (open circles) as a function of log of reduced surface pressure ($\pi_c - \pi$) at 70% DMPC/30% DChol. Points represent the average and standard deviation of 9–13 domains per pressure. (B) Effective line tension $\gamma_{eff} = \gamma - \mu^2$ as a function of surface pressure derived using our results (open circles) compared with previously published data (filled diamonds, ref 29; filled squares, ref 32). (C) Normalized γ (black) and μ^2 (lined) and standard deviation calculated from 500 frame sequences of 10 domains at $\pi = 9$ mN/m. Values for each domain were normalized to the average γ and μ^2 of all 10 domains as calculated using the first 500 frames of each domain. (D) γ (filled diamonds) and μ^2 (open circles) as a function of domain radius at $\pi = 9$ mN/m (top left), 8.75 mN/m (top right), 8.5 mN/m (bottom left), and 8.25 mN/m (bottom right).

Results

Mixed monolayer membranes of DMPC and DChol at the critical composition (70% DMPC/30% DChol) were imaged at a range of surface pressures decreasing from the critical pressure (10.1 mN/m) down to a pressure of 6.5 mN/m. Our critical pressure is in good agreement with published values.[52] Image frames were analyzed to extract the bare line tension γ and dipole density difference μ as a function of surface pressure as described above. Both γ and μ decreased from 0.64 to 0.22 pN and 0.68 to 0.44 D/100 Å^2, respectively, as the surface pressure was increased from 6.5 to 9 mN/m (Figure 2A). The pressure dependence of line tension and dipole density difference, near the critical point, can be expressed as a function of the critical exponents d and β, respectively.[29,53] These relations are $\gamma = m\pi_r^d$ and $\mu = n\pi_r^{2\beta}$, where m and n are adjustable parameters and the reduced surface pressure $\pi_r = \pi_c - \pi$; that is, π_r is the deviation of the film pressure from the critical pressure π_c. For the critical composition, the exponents for the dependence of γ and μ^2 on reduced surface pressure were 0.9 ± 0.22 and 0.35 ± 0.09, respectively (see Figure 3C). These values compare favorably with those assumed by Benvegnu and McConnell (1.0 and 0.33, respectively). The largest contribution to the uncertainty in our critical exponents stems from the uncertainty of the measurement of π_c (± 0.5 mN).

The effective line tensions obtained from the relation $\gamma_{eff} = \gamma - \mu^2$ measured here are in excellent agreement with those previously derived from the recovery of domain shape following external distortion (see Figure 2B and ref 29). Note, however, that the discussion in ref 29 indicates a small uncertainty in their measured values due to approximations inherent in their
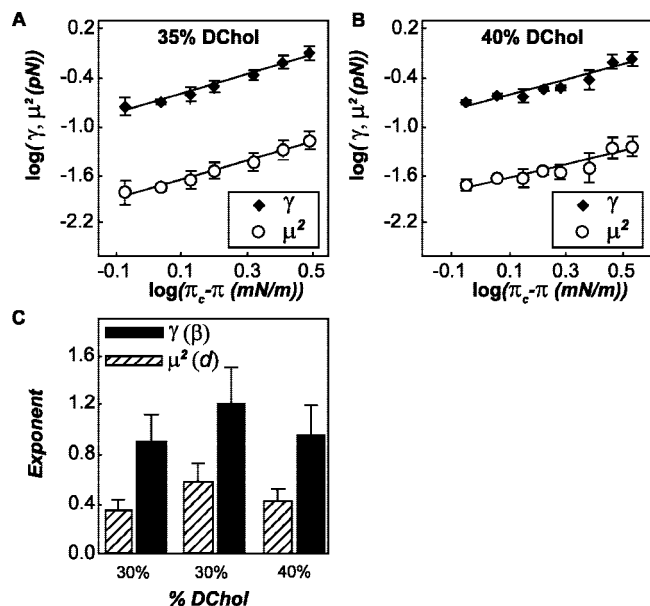
Lipid Monolayer Domain Boundary Fluctuations

J. Phys. Chem. B, Vol. 112, No. 27, 2008 **8067**

Figure 3. Composition dependence of line tension and dipole density difference. (A) Same as Figure 2A at 65% DMPC/35% DChol. Points represent the average ± standard deviation of 6−10 domains per pressure. (B) Same as Figures 2A and 3A at 60% DMPC/40% DChol. Points represent the average ± standard deviation of 10−14 domains per pressure. (C) Exponents for γ (black) and μ^2 (lined) as a function of monolayer composition. Exponents calculated from slopes of linear fits to data in Figures 2A and 3A,B. Error bars reflect the 25% uncertainty in exponents resulting from a 0.5 mN/m error in transition pressure.

analysis approach. Hence, the remarkable agreement of our findings with those of ref 29 could be somewhat fortuitous.

Additionally, γ and μ measured by Goldstein and Jackson from a preliminary data set near the critical pressure match the trends observed with our data (quantitative differences could be due to their data being taken closer to the critical point[30]). A recent capillary wave theory quantification of γ_{eff}[32] measured a very similar line tension at high surface pressure (8.3 mN/m), although a significantly different surface pressure dependence (see Figure 2B) of γ was observed.

Measurement of 2000 consecutive frames for each domain allowed us to quantify the effect of photoinduced oxidation on the measured parameters of γ and μ. Both parameters were reduced by ∼10%, which was a statistically insignificant amount, when calculated from the third and fourth sets of 500 frames (<10 s) of the sequences compared with the first or second (Figure 2C). This reduction was associated with significant photobleaching and might be suggestive of photoinduced generation of line active oxidation products. This observation is in accordance with the observed reduction of line tension by photoinduced production of cholestenone in a similar mixed monolayer.[50] Note, however, that since both γ and μ are affected by photobleaching products, these appear to have an effect not only on phase boundary properties but also on the bulk properties of the coexisting domains.

The large number of domains analyzed in this report allowed quantification of the dependence of line tension on domain size. Surprisingly, a correlation was found between the radius and the γ and μ values obtained for each domain, with a slight reduction in both parameters with increasing domain size (see the examples of four different pressures in Figure 2D). Although the data from a single pressure were quite spread, normalizing all data sets to a single surface pressure using the critical

exponents showed the dependence to be significant to a p value of 0.05 for μ and 0.06 for γ.

In addition to quantification of critical exponents for line tension and dipole density difference at the critical composition (30% DChol), these parameters were measured at 35% and 40% DChol, compositions that lie in the same binary miscibility gap as the 30% sample, and domain edge fluctuations were observed for these additional mixtures as expected from the monolayer phase diagram.[10] Although a trend of γ and μ decreasing with surface pressure was observed for all compositions and all data sets were fit well by power laws, the quantitative relationships between these parameters were not identical (Figure 3A,B). The critical exponents at 35% DChol were 1.2 for γ and 0.6 for μ^2, significantly higher than those for either 30% or 40% (Figure 3C). Since these critical exponents are strongly dependent on exact quantification of the transition pressure of the monolayer, it is difficult to confidently ascribe a trend to these observations.

Discussion

An advance of the present contribution is the analysis of a large data set in the framework of the Goldstein and Jackson (GJ) theory to independently measure dipole density difference and line tension in coexisting liquid phases to determine critical exponents for the variation of these parameters as a function of surface pressure. Our data included at least 1000 image frames per domain, 10 domains at each pressure, 6−7 surface pressures per composition, and 3 different compositions. This data volume allowed both confident determinations of average γ and μ values at each pressure, as well as quantification of the domain-to-domain variability in these measurements. The magnitudes of the measured parameters agree remarkably well with previously published values,[29] especially considering the difference in the approaches used to derive them. It is interesting to note that the two-dimensional Ising model predicts a value of 1/8 for the exponent, β.[53] Hirshfeld and Seul,[17] however, found the shape of their mixed monolayer phase coexistence boundary to be in better agreement with an exponent of 1/3, the Ising model exponent for three dimensions,[53] and Hagen and McConnell obtained $\beta = 0.25 \pm 0.7$ from a set of different mixtures.[54] As discussed in ref 54, despite the molecular thickness of monolayer films, intermolecular interactions in a lipid monolayer are not truly two-dimensional, which may explain the deviation from the 2D Ising model expectation.

An important distinction between our data and previously published results is the quantification of bare versus effective line tension. Previous estimates of line tension in monolayers by physical perturbations[29,31] have measured γ_{eff}, which includes both the bare line tension (γ) quantified here and the dipolar repulsive effects: $\gamma_{eff} = \gamma - \mu^2$. For our measurements, dipolar contributions to effective line tension were 7−9%, increasing slightly with film pressure for all compositions. It seems plausible that line active components could affect γ without modifying μ thereby changing the interdependence of these parameters.[55]

The photobleaching effect suggested by our experiments was not unexpected, since previous work cited a line tension reducing effect of cholestenone produced by the photoinduced oxidation of cholesterol.[50] Although dihydrocholesterol was used in our studies to prevent oxidative effects,[50] this cholesterol analog can be oxidized to cholestanone[56] with a similar structure to cholestenone, which could have similar line active properties. We included 5 mM DTT in the subphase to minimize photobleaching with the aim of maximizing the number of image frames that could be analyzed. Without DTT addition, the

Heinrich et al.

illuminated area of the monolayer was bleached within 15 s (referring to less than 1000 frames) to the point that boundary tracing by thresholding became inaccurate. It is interesting to note that photobleaching products appear to have the opposite effect (i.e., lead to an increase in line tension) in bilayer vesicles, as recently found by flicker spectroscopy in GUVs.[33]

A further point of note is the composition dependence of the measured parameters γ and μ^2. The exponents for the relationship of these parameters to film pressure for all compositions were similar to the 1.0 for γ and 0.33 for μ^2 predicted by Benvegnu and McConnell,[29] but there was an apparent increase in these exponents at noncritical concentrations. However, these exponents depend strongly on the experimental value for the transition pressure, which is observation-dependent, with ~25% variation in exponents expected with a 0.5 mN/m error in transition pressure. Thus, although we observed composition-dependent variations in exponents, a systematic trend in the concentration dependence could not be deduced from our data set.

An unexpected finding enabled by the large data set used in these experiments was the domain size dependence of line tension and dipole density difference. Equation 6 predicts domain shape instability for domain radii that approach a critical value. It is possible that, as experimental domain radii get closer to the critical radius for the first instable mode, the capillary wave theory of GJ becomes increasingly inaccurate since fluctuations may transiently probe unstable regimes near the shape transition. This hypothesis awaits more systematic experimental investigation.

Conclusion

By examining thermally induced fluctuations of domain boundaries in mixed monolayers of DMPC and DChol, we were able to independently quantify line tension and dipole density differences between coexisting fluid monolayer domains. These parameters were dependent on a reduced pressure, expressed as the difference between film pressure and the miscibility transition pressure, with the exponents closely matching those predicted by previous estimates. We believe that the method of flicker spectroscopy could contribute to the identification of line active biologically relevant components.

References and Notes

(1) Simons, K.; Ikonen, E. *Nature* **1997**, *387*, 569.
(2) Dietrich, C.; Bagatolli, L. A.; Volovyk, Z. N.; Thompson, N. L.; Levi, M.; Jacobson, K.; Gratton, E. *Biophys. J.* **2001**, *80*, 1417.
(3) Samsonov, A. V.; Mihalyov, I.; Cohen, F. S. *Biophys. J.* **2001**, *81*, 1486.
(4) Korlach, J.; Schwille, P.; Webb, W. W.; Feigenson, G. W. *Proc. Natl. Acad. Sci. U.S.A.* **1999**, *96*, 8461.
(5) Bagatolli, L. A.; Gratton, E. *Biophys. J.* **2000**, *78*, 290.
(6) Von Tscharner, V.; McConnell, H. M. *Biophys. J.* **1981**, *36*, 409.
(7) Losche, M.; Sackmann, E.; Mohwald, H. *Berichte Der Bunsen-Gesellschaft-Physical Chemistry Chemical Physics* **1983**, *87*, 848.
(8) Veatch, S. L.; Keller, S. L. *Biochim. Biophys. Acta* **2005**, *1746*, 172.
(9) McConnell, H. M. *Annu. Rev. Phys. Chem.* **1991**, *42*, 171.

(10) Okonogi, T. M.; McConnell, H. M. *Biophys. J.* **2004**, *86*, 880.
(11) Subramaniam, S.; McConnell, H. M. *J. Phys. Chem.* **1987**, *91*, 1715.
(12) Keller, S. L.; Anderson, T. G.; McConnell, H. M. *Biophys. J.* **2000**, *79*, 2033.
(13) Baumgart, T.; Hess, S. T.; Webb, W. W. *Nature* **2003**, *425*, 821.
(14) Veatch, S. L.; Keller, S. L. *Phys. Rev. Lett.* **2002**, *89*, 268101.
(15) Veatch, S. L.; Keller, S. L. *Biophys. J.* **2003**, *85*, 3074.
(16) Subramaniam, S.; McConnell, H. *J. Phys. Chem.* **1987**, *91*, 1715.
(17) Hirshfeld, C. L.; Seul, M. *J. Phys.* **1990**, *51*, 1537.
(18) Hammond, A. T.; Heberle, F. A.; Baumgart, T.; Holowka, D.; Baird, B.; Feigenson, G. W. *Proc. Natl. Acad. Sci. U.S.A.* **2005**, *102*, 6320.
(19) Veatch, S.; Soubias, O.; Keller, S. L.; Gawrisch, K. *PNAS* **2007**, *104*, 17650.
(20) Heberle, F. A.; Buboltz, J. T.; Stringer, D.; Feigenson, G. W. *Biochimica Et Biophysica Acta-Molecular Cell Research* **2005**, *1746*, 186.
(21) Silvius, J. R. *Biophys. J.* **2003**, *85*, 1034.
(22) Nielsen, L. K.; Bjornhom, T.; Mouritsen, O. G. *Nature* **2000**, *404*, 352.
(23) Radhakrishnan, A.; McConnell, H. *J. Chem. Phys.* **2007**, 126.
(24) Baumgart, T.; Hammond, A. T.; Sengupta, P.; Hess, S. T.; Holowka, D.; Baird, B.; Webb, W. W. *PNAS* **2007**, *104*, 3165.
(25) Frolov, V. A. J.; Chizmadzhev, Y. A.; Cohen, F. S.; Zimmerberg, J. *Biophys. J.* **2006**, *91*, 189.
(26) Baumgart, T.; Das, S.; Webb, W. W.; Jenkins, J. T. *Biophys. J.* **2005**, *89*, 1067.
(27) Tian, A.; Johnson, C.; Wang, W.; Baumgart, T. *Phys. Rev. Lett.* **2007**, *98*, 208102.
(28) Liu, J.; Kaksonen, M.; Drubin, D. G.; Oster, G. *Proc. Natl. Acad. Sci. U.S.A.* **2006**, *103*, 10277.
(29) Benvegnu, D. J.; McConnell, H. M. *J. Phys. Chem.* **1992**, *96*, 6820.
(30) Goldstein, R. E.; Jackson, D. P. *J. Phys. Chem.* **1994**, *98*, 9626.
(31) Wurlitzer, S.; Steffen, P.; Fischer, T. M. *J. Chem. Phys.* **2000**, *112*, 5915.
(32) Stottrup, B. L.; Heussler, A. M.; Bibelnieks, T. A. *J. Phys. Chem. B* **2007**, *111*, 11091.
(33) Esposito, C.; Tian, A.; Melamed, S.; Johnson, C.; Tee, S. Y.; Baumgart, T. *Biophys. J.* **2007**, *93*, 3169.
(34) Blanchette, C. D.; Lin, W. C.; Orme, C. A.; Ratto, T. V.; Longo, M. L. *Langmuir* **2007**, *23*, 5875.
(35) Zou, L.; Wang, J.; Basnet, P.; Mann, E. K. *Phys. Rev. E* **2007**, *76*.
(36) Wintersmith, J. R.; Zou, L.; Bernoff, A. J.; Alexander, J. C.; Mann, J. A.; Kooijman, E. E.; Mann, E. K. *Phys. Rev. E* **2007**, *75*.
(37) Alexander, J. C.; Bernoff, A. J.; Mann, E. K.; Mann, J. A.; Wintersmith, J. R.; Zou, L. *J. Fluid Mech.* **2007**, *571*, 191.
(38) McConnell, H. M.; Rice, P. A.; Benvegnu, D. J. *J. Phys. Chem.* **1990**, *94*, 8965.
(39) Klingler, J. F.; Mcconnell, H. M. *J. Phys. Chem.* **1993**, *97*, 2962.
(40) Seul, M.; Sammon, M. J. *Phys. Rev. Lett.* **1990**, *64*, 1903.
(41) Langer, S. A.; Goldstein, R. E.; Jackson, D. P. *Phys. Rev. A* **1992**, *46*, 4894.
(42) McConnell, H. M. *J. Phys. Chem.* **1990**, *94*, 4728.
(43) Deutch, J. M.; Low, F. E. *J. Phys. Chem.* **1992**, *96*, 7097.
(44) Stone, H. A.; Mcconnell, H. M. *Proc. R. Soc. London Ser. A: Math. Phys. Sci.* **1995**, *448*, 97.
(45) Lee, K. Y. C.; McConnell, H. M. *J. Phys. Chem.* **1993**, *97*, 9532.
(46) Heinrich, M; Levental, I; Gelman, H; Janmey, P; Baumgart, T. *J. Phys. Chem. B* **2008**, . submitted.
(47) Lubensky, D. K.; Goldstein, R. E. *Physics of Fluids* **1996**, *8*, 843.
(48) Kates, M. *Techniques of Lipidology 2nd ed.*; Elsevier Science Publishers B.V: Amsterdam, 1986.
(49) Stottrup, B. L.; Keller, S. L. *Biophys. J.* **2006**, *90*, 3176.
(50) Benvegnu, D.; McConnell, H. *J. Phys. Chem.* **1993**, *97*, 6686.
(51) Seul, M.; Sammon, M. J.; Monar, L. R. *Rev. Sci. Instrum.* **1991**, *62*, 784.
(52) Keller, S. L.; Radhakrishnan, A.; McConnell, H. M. *J. Phys. Chem. B* **2000**, *104*, 7522.
(53) Rowlinson J. S.; Widom B. *Molecular Theory of Capillarity*; Clarendon Press: Oxford, 1982.
(54) Hagen, J. P.; McConnell, H. M. *Biochimica Et Biophysica Acta-Biomembranes* **1997**, *1329*, 7.
(55) Trabelsi, S.; Zhang, S.; Lee, T. R.; Schwartz, D. K. *Phys. Rev. Lett.* **2008**, 1.
(56) Grimalt, J. O.; Fernandez, P.; Bayona, J. M.; Albaiges, J. *Environ. Sci. Technol.* **1990**, *24*, 357.